RNA (1997), 3:291-302. Cambridge University Press. Printed in the USA.

In vitro RNA binding of the hepatitis A virus proteinase 3C (HAV $3C^{pro}$) to secondary structure elements within the 5′ terminus of the HAV genome

YURI Y. KUSOV and VERENA GAUSS-MÜLLER
Institute of Medical Molecular Biology, Medical University of Lübeck, D-23538 Lübeck, Germany

ABSTRACT

The secondary structure elements at the 5′ nontranslated region (NTR) of the picornaviral RNAs can be divided functionally into two domains, one of which directs cap-independent translation, whereas the other is essential for viral RNA replication. For the latter, the formation of an RNA replication complex that involves particularly viral proteinase-containing polypeptides and cellular proteins has been shown (Andino R, Rieckhof GE, Achacoso PL, Baltimore D, 1993, *EMBO J 12*:3587–3598; Xiang W et al., 1995, *RNA 1*:892–904). To initiate studies on the formation of the hepatitis A virus (HAV) RNA replication complex, binding of the HAV proteinase $3C^{pro}$ and 3CD to secondary structure elements at the 5′ and 3′ NTR of the HAV RNA was investigated. Using mobility shift assay, UV crosslinking/label transfer, and northwestern analysis, we show that both the HAV $3C^{pro}$ and the proteolytically inactive mutant bind to in vitro synthesized transcripts, suggesting that the RNA-binding site of the enzyme is separated spatially from its catalytic center. Weak interactions with HAV $3C^{pro}$ were found for individual secondary structure elements comprising less than 100 nt. RNA-binding specificity was unambiguous for transcripts comprising at least two stem-loops along with the polypyrimidine tract. Furthermore, competition experiments suggest that the 5′ terminus of the HAV genome contains multiple binding sites for HAV $3C^{pro}$. In contrast to poliovirus, binding capacity of HAV 3CD to RNA of the 5′ NTR was not improved as compared to 3C. The data imply that, during the viral life cycle, HAV $3C^{pro}$ might serve replicative function(s) in addition to proteolysis of the viral polyprotein.

Keywords: cloverleaf; mobility shift; picornavirus; polypyrimidine; RNA replication; stem-loop; UV crosslinking

INTRODUCTION

The RNA genome of picornaviruses consisting of 7,000–8,000 nt is of messenger polarity and contains one open reading frame coding for a polyprotein, which is flanked on either side by *cis*-acting, nontranslated regions (NTR). Following virus penetration into the cell, the viral genome is translated into a polyprotein of more than 200 kDa. Translation is cap-independent by virtue of a portion of the 5′ NTR that folds into highly structured elements serving as an internal ribosomal entry site (IRES). By proteolytic cleavages of the primary translation product, about a dozen viral proteins are released that fulfil various functions. Polyprotein processing, which is a prime regulatory step in viral gene expression, has been studied intensively for poliovirus, the picornaviral prototype (reviewed in Wimmer et al., 1993). Besides the primary and maturation cleavages, all proteolytic steps are catalyzed by the major viral proteinase $3C^{pro}$, which by itself is a part of the polyprotein. It is active in its mature form and also as precursor polypeptide $3CD^{pro}$ fused to the viral polymerase or as protein 3ABC fused to the anchor-bound primer 3AB (Ypma-Wong et al., 1988; Jackson, 1989). In contrast to other picornaviruses, the hepatitis A virus (HAV) protein $3C^{pro}$ is the only virus-encoded proteinase that catalyzes primary and secondary processing steps (Jia et al., 1991; Schultheiss et al., 1994). Like other picornaviral 3C proteins, HAV $3C^{pro}$ is a cysteine proteinase with structural homologies to the chymotrypsin family (Bazan & Fletterick, 1988; Gorbalenya et al., 1989). HAV and rhinovirus $3C^{pro}$ have been crystallized and their three-dimensional structure has been determined (Allaire et al., 1994; Matthews et al., 1994), which has opened the way for the rational design of antiviral strategies. Mutational analysis confirmed the active site and suggested a putative RNA-binding domain.

Reprint requests to: Yuri Kusov, Institute of Medical Molecular Biology, Medical University of Lübeck, Ratzeburger Allee 160, 23538 Lübeck, Germany; e-mail: koussov@molbio.mu-luebeck.de.

Following or simultaneous with RNA translation and polyprotein processing, the viral plus-strand genome serves as a template for viral RNA replication, which is mediated by the viral polymerase $3D^{Pol}$ and supported by other viral and host proteins. To initiate minus-strand RNA synthesis, a complex involving secondary structure elements at the 3′ end of the viral genome is presumably formed (Jacobson et al., 1993; Harris et al., 1994; Kusov et al., 1996). The minus strand, in particular in its double-stranded replicative form, is utilized for de novo synthesis of plus strands. The highly structured RNA elements at the 5′ end of the plus strand might be the nucleation point for the formation of a replication initiation complex consisting of several viral and host proteins (Andino et al., 1993; Harris et al., 1994). In fact, it was shown that the 5′-terminal 90 nt of the polio and rhinovirus genome form a cloverleaf-like structure that interacts specifically with viral proteins $3C^{pro}$, 3CD, and 3AB (Andino et al., 1990; Leong et al., 1993; Harris et al., 1994; Walker et al., 1995; Xiang et al., 1995a). Additional evidence for the role of the 5′ cloverleaf and its interaction with compatible viral proteins in RNA replication came from studies with viral replicons (Percy et al., 1992; Rohll et al., 1994).

Like other picornaviruses, the HAV 5′ NTR can be divided into two functional domains, the larger of which is the HAV IRES and comprises nt 151–734 (Brown et al., 1991) or 100–734 (Carneiro et al., 1995). This RNA region interacts with host proteins and ensures cap-independent translation, albeit not as efficiently as that of other picornaviruses (Chang et al., 1993; Brown et al., 1994; Whetter et al., 1994; Borman et al., 1995). In contrast to entero- and rhinoviruses, the smaller domain, consisting of the 5′-most 150 nt of the HAV genome, comprises three stem-loops and a polypyrimidine tract (pY1) (Brown et al., 1991; Le et al., 1993). Genetic analysis suggested that pY1 might be functionally similar to the cardiovirus polycytidine tract because both seem to be essential for viral RNA replication in vivo but not in vitro (Shaffer et al., 1994; Hahn & Palmenberg, 1995; Shaffer & Lemon, 1995; Martin et al., 1996).

To assess the role of the 5′-terminal HAV RNA structures in RNA replication and in the formation of a replication complex, we initiated in vitro studies on the interaction of RNA transcripts with viral proteins. Here we show that HAV $3C^{pro}$ is an RNA-binding protein with specificity for the most 5′-terminal RNA structures of the HAV genome. Because more than one secondary structure element is required for efficient interaction, multiple RNA-binding sites on HAV $3C^{pro}$ can be assumed. RNA interaction is not abolished in the proteolytically inactive enzyme, implying that the RNA-binding region is located in an area distinct from the catalytic triad. The data suggest that HAV 3C might serve multiple, yet unknown, functions during the viral life cycle.

RESULTS

Expression, purification, and label transfer to HAV $3C^{pro}$ and 3CD

Some picornaviral nonstructural proteins have been proposed to exert multiple functions during the course of the infectious cycle (see Wimmer et al., 1993 for review). To assess potential function(s) of HAV $3C^{pro}$ apart from its proteolytic role in the liberation of viral proteins from the polyprotein, the RNA-binding activity of 3C and 3CD was tested. The active HAV proteinase $3C^{pro}$ and its proteolytically inactive mutant $3C\mu$ (C24S and C172A) were expressed in *Escherichia coli* and purified by ion-exchange chromatography to near homogeneity (Fig. 1A, lane 1). Purification of proteolytically inactive 3CD (C172A) was performed by metal affinity chromatography (not shown). Interaction with RNA secondary structure elements at the 5′ end of the HAV genome was determined using various methods. Incubation with the radioactively labeled transcript representing element IV (see Fig. 2) followed by UV cross-linking showed that label was transferred from RNA to HAV $3C^{pro}$ (Fig. 1B, lane 1). RNA binding of 3C was specific because neither the heat-denatured protein nor bovine serum albumin (BSA) interacted (Fig. 1B, lanes 2 and 3, respectively). Binding of viral RNA I–V (see Fig. 2) to HAV $3C^{pro}$, but not to BSA, was also demonstrated by northwestern blot (Fig. 1C, lanes 1 and 2). Both the RNA-free as well as the RNA-bound proteinase was reactive with anti-3C, which was obvious from immunoblot and northwestern analysis, respectively (Fig. 1A, lane 2 and Fig. 1C, lane 3). BSA used as a negative control was not detected by anti-3C (Fig. 1C, lane 4), whereas the mutated enzyme $3C\mu$ reacted as well (data not shown). Label transfer from RNA I-V to HAV $3C\mu$ was similar to what is shown in lane 1, Figure 1B, implying that perturbation of the catalytic site does not interfere with RNA binding. RNA-binding activity of proteolytically inactive HAV 3CD was assayed in a similar manner and found to be highly specific because label of the RNA probe representing the 3′ NTR was transferred only to the expected protein of approximately 80 kDa (Fig. 1D, lane 2), which was immunologically reactive with anti-3C (lane 1) and anti-3D (not shown). Some additional anti-3C reactive proteins (lane 1) probably represent the 3CD-degradation products.

5′ NTR secondary structure elements represented by HAV RNA probes

Like cardio- and aphthoviruses (Rueckert, 1996), HAV RNA does not form a cloverleaf at its 5′ end, but rather a stem-loop structure (Iabc), separated from the IRES by a polypyrimidine tract (Id, see Brown et al., 1991). To test whether this and/or other secondary structure elements of the HAV 5′ NTR, depicted schematically in Fig-

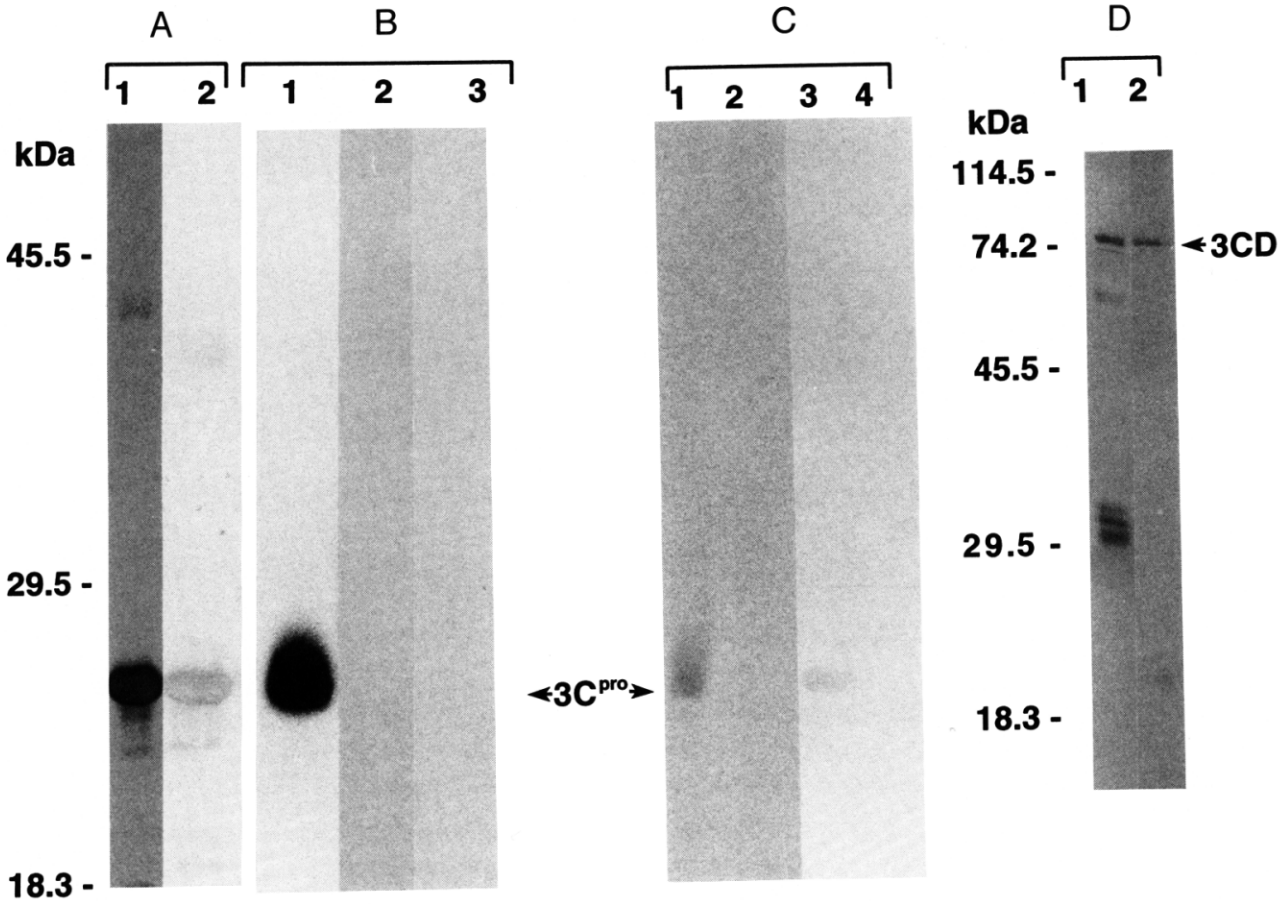

FIGURE 1. RNA-binding activity of recombinant HAV 3C^{pro}. **A:** Bacterially expressed HAV 3C^{pro} protein was purified and analyzed by SDS-PAGE followed by silver staining (lane 1) and immunoblot using anti-3C (lane 2). Silver staining and immunoblot of purified mutant enzyme 3Cμ were identical. **B:** Label transfer from HAV RNA IV (nt 355–532, see Fig. 2) to HAV 3C^{pro} (lane 1), heat-denatured HAV 3C^{pro} (lane 2), and BSA (lane 3) after RNA-binding reaction, UV crosslinking, and RNase digestion. The radioactive products were examined by SDS-PAGE followed by autoradiography. **C:** Northwestern analysis. Five micrograms of purified HAV 3C^{pro} (lane 1) or BSA (lane 2) were separated by SDS-PAGE, transferred onto a nitrocellulose membrane (Schleicher & Schüll), renatured by incubating in decreasing amounts of guanidinium hydrochloride, probed with radioactive RNA I–V (nt 1–744, see Fig. 2), and autoradiographed. After autoradiography, HAV 3C^{pro} (lane 3) and BSA (lane 4) were tested by immunological reaction with anti-3C. The mobility of HAV 3C^{pro} and protein markers are shown. **D:** Bacterially expressed HAV 3CD was purified by a Ni-NTA column and analyzed by immunoblot with anti-3C (lane 1). Label transfer from RNA representing the 3′ NTR of the HAV genome (nt 7414–7502, see Fig. 2) to HAV 3CD after RNA-binding reaction, UV crosslinking, and RNase digestion, followed by SDS-PAGE and autoradiography (lane 2). The mobility of protein markers and that of 3CD are indicated.

ure 2A, interact with HAV proteinase 3C^{pro}, a panel of RNA probes was created (Fig. 2B). By restricting the HAV full-length cDNA at sites within the 5′ NTR, we were able to prepare transcripts encompassing various secondary structure elements individually or in combinations. Transcripts shortened progressively at the 3′ end are denoted I–V for the entire 5′ NTR, I–III and I–II for the truncated elements. RNAs with progressive 5′ deletions included elements Ib–V, II–V, IV–V, IV*–V, V, and V*. The RNAs comprising nt 151–248, 151–354, and 355–532, and representing secondary structure elements II, II–III, and IV, respectively, were transcribed from HAV cDNAs deleted progressively at the 5′ end. The 5′-most element I is represented by RNA Iabcd, which is composed of three stem-loops, Ia, Ib, Ic, and a polypyrimidine tract (Id) of approximately 40 nt (HAV RNA148). These elements were also prepared individually or in combinations (Iab, Iabc, and Ibcd). The specificity of RNA–protein interaction was assessed by using control RNA probes that represented the 3′ NTR of HAV, the 5′ cloverleaf of poliovirus type 1 (Mahoney) RNA (PV(M) RNA108), and the 5′ cloverleaf of human rhinovirus 14 RNA (HRV14 RNA126). The impact of vector-derived sequence on interaction with HAV 3C^{pro} was estimated by using a transcript from the multiple cloning site of pGEM1 (pGEM1-mcs).

Interaction of HAV 3C^{pro} with transcripts representing various parts of the HAV 5′ NTR

Previously, it has been shown that various parts of the HAV 5′ NTR interact specifically with cellular pro-

A

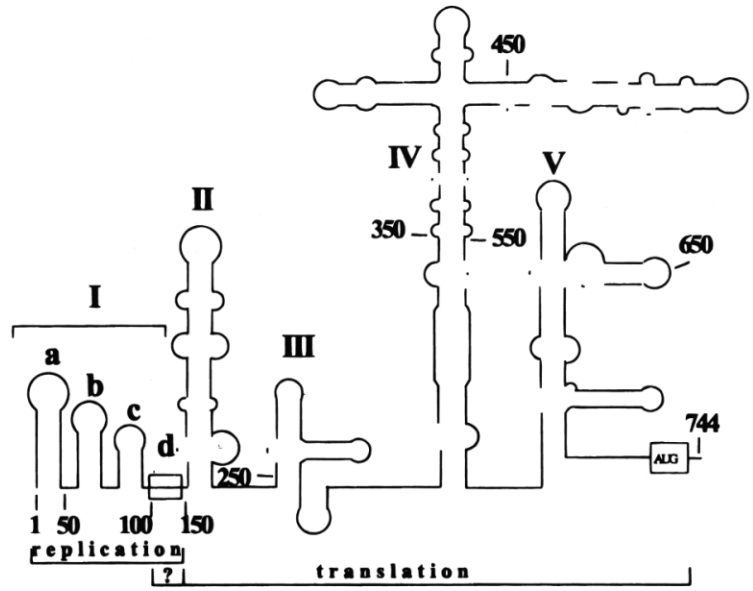

B

Secondary-structure element(s) within RNA probe	Nucleotide position	Length (nt) viral	total	Interaction with HAV 3C^{pro}
Ia	1-45	45	52	-
Ib	46-81	36	43	-
Ic	81-95	15	27	-
Id	96-148	53	65	-
Iab	1-81	81	88	-
Iabc	1-95	95	107	+/-
Iabcd	1-148	148	155	+
Ibcd	46-148	103	110	+
I - II	1-248	248	255	++
I - III	1-354	354	361	++
I - V	1-744	744	751	++
Ib - V	46-744	699	706	++
II	151-248	98	105	+/-
II - III	151-354	204	211	+
II - V	151-744	594	601	++
IV	355-532	178	185	++
IV - V	355-744	390	397	++
IV* - V	447-744	298	305	++
V	533-744	212	219	++
V*	634-744	111	118	+/-
Control RNAs:				
HAV 3`NTR	7414-7502	89	117	-
PV1(M) RNA108	1-108	108	110	-
HRV14 RNA126	1-126	126	126	-
pGEM1-mcs	1-51	-	52	-

FIGURE 2. **A:** Schematic representation of the HAV RNA secondary structure at the 5′ NTR. The nucleotide position is indicated. The first AUG codon and the polypyrimidine tract (element Id, approximately 40 nt) are indicated by the open boxes. **B:** Secondary structure elements, nucleotide position, and length (nt) of the RNA probes used are shown. Their interaction with HAV 3C^{pro} is represented by "−" (neither mobility shift nor label transfer) or by "+" and "++" (partial and complete mobility shift, respectively). "+/−" corresponds to mobility shift not detectable as distinct band.

teins, one of which was identified recently as glyceraldehyde 3-phosphate dehydrogenase (Chang et al., 1993; Schultz et al., 1996). On the other hand, direct binding of human rhinoviral 3C^{pro} to its cognate 5′ end RNA was also demonstrated (Leong et al., 1993; Walker et al., 1995). To find out whether HAV 3C^{pro} interacts with secondary structure elements within the HAV 5′ NTR, mobility shift and UV crosslinking/label transfer assays were performed using RNA transcripts representing various parts of the HAV 5′ NTR. To prevent nonspecific RNA–protein interaction, all binding reactions were conducted in the presence of a more than 1,000-fold molar excess of unlabeled tRNA. The experiments presented below show the RNA interaction of the wild-type HAV 3C^{pro}. Because identical results were obtained for the proteolytically inactive

enzyme, it can be concluded that both wild-type and mutated HAV 3C^{pro} are RNA-binding proteins. As shown in Figure 3, RNA probes corresponding to the first stem-loops of the 5′ NTR (Ia and Iab) did not interact with 3C^{pro} because neither their electrophoretic mobilities were retarded in the presence of HAV 3C^{pro} (Fig. 3B, lanes 1–4) nor was the RNA label transferred to the protein after UV crosslinking followed by RNase digestion (Fig. 3A, lanes 2 and 4). HAV 3C^{pro} formed a ribonucleoprotein (RNP) complex with the RNA represented by the element Iabcd (Fig. 3B, lanes 5 and 6). This RNA was also able to transfer the label to

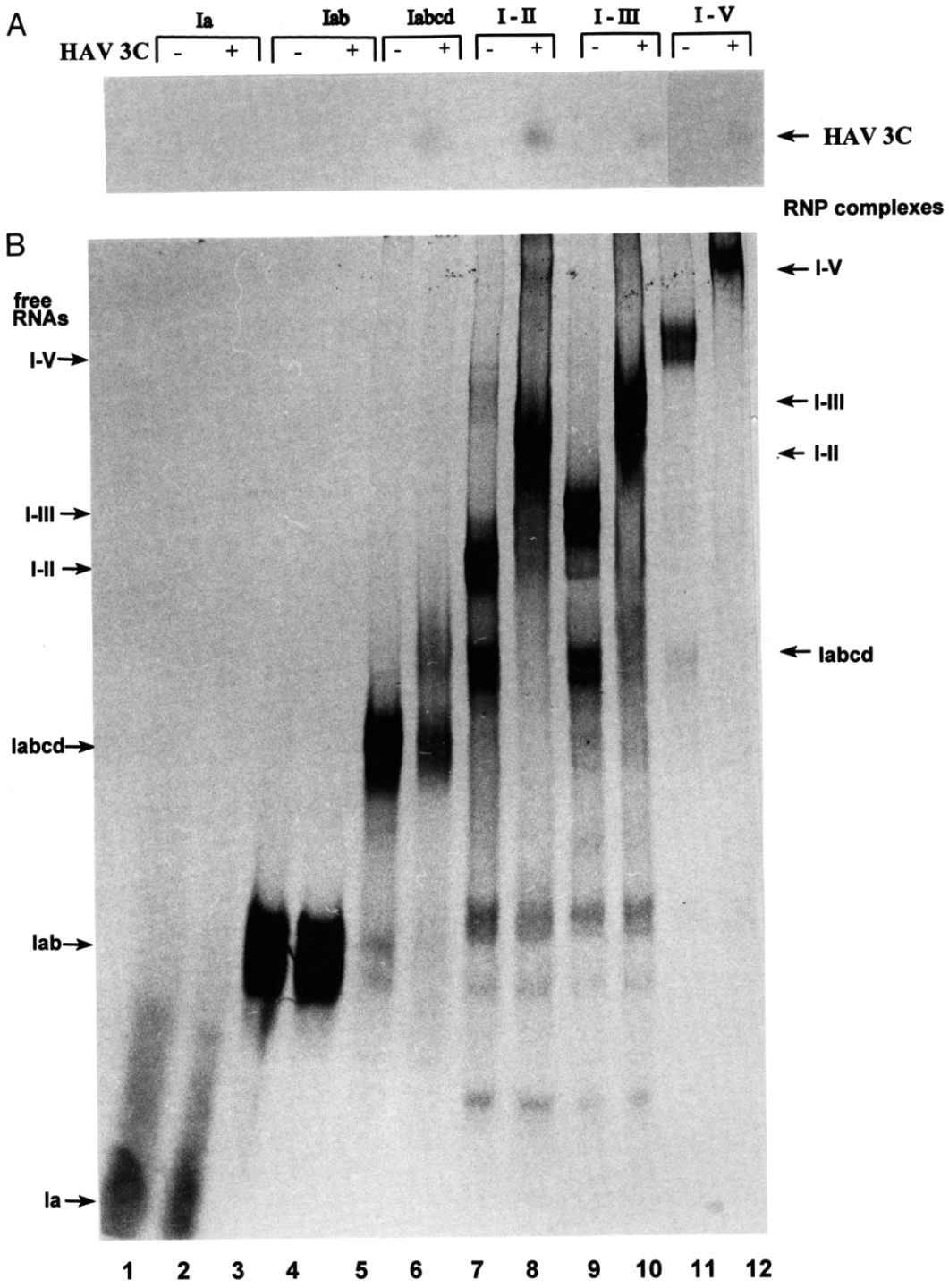

FIGURE 3. Interaction of HAV 3C^{pro} with 3′ progressively deleted transcripts derived from the HAV 5′ NTR. **A:** Label transfer to HAV 3C^{pro} (+) from the indicated free radioactive RNA probes (−). **B:** Mobility of free RNA probes (left) and their RNP complexes with HAV 3C^{pro} (+) analyzed by native PAGE. The transcripts migrating faster than the free RNA probes represent prematurely terminated products.

HAV $3C^{pro}$, albeit not efficiently (Fig. 3A, lane 6). All RNA probes comprising more than 150 nt induced a complete shift of RNA mobility and transferred the label to HAV $3C^{pro}$ (Fig. 3, lanes 7–12). 5′ Progressively deleted transcripts, as well as individual secondary structure elements or their combinations within the HAV IRES, were tested similarly and found to interact with $3C^{pro}$ (summarized in Fig. 2B). The RNA transcripts migrating either faster or slower than the free probes might represent prematurely terminated products (Fig. 3B, lanes 5–11).

Specificity of the $3C^{pro}$ interaction at the 5′ end of the HAV RNA

To determine the minimal RNA region needed for HAV $3C^{pro}$ binding, RNA probes representing individual secondary structure elements at the 5′ end of the HAV RNA or combinations thereof were prepared from PCR-amplified cDNAs and used in binding assays. As shown in Figure 4, neither stem-loops Ib and Ic nor the polypyrimidine tract Id were retarded by HAV $3C^{pro}$ in the mobility shift assay (lanes 1–6). RNA Iabc, containing three stem-loops, interacted only weakly with the protein, as follows from a smear above the RNA probe (lane 10). Interaction of 3C with element Ibcd led to a complete mobility shift (lanes 7 and 8). An RNA probe of approximately the same length as Ibcd and representing the two stem-loops of the HAV 3′ NTR did not bind to HAV $3C^{pro}$ (lanes 11 and 12; see also Kusov et al., 1996). Taken together, the data presented in Figures 3 and 4 demonstrate that HAV $3C^{pro}$ is able to form stable gel-resolvable complexes with RNAs that contain at least two of the 5′ end stem-loop elements along with the polypyrimidine tract (Iabcd, Fig. 3, lane 6 and Ibcd, Fig. 4, lane 8), whereas weak interaction occurs with RNAs encompassing only portions of these structures (Iabc, Fig. 4, lane 10).

For poliovirus, 3CD interaction with the cognate 5′ cloverleaf was found to be at least 10 times stronger than that of 3C (Andino et al., 1993). To compare the RNA-binding activity of HAV 3C with that of 3CD, var-

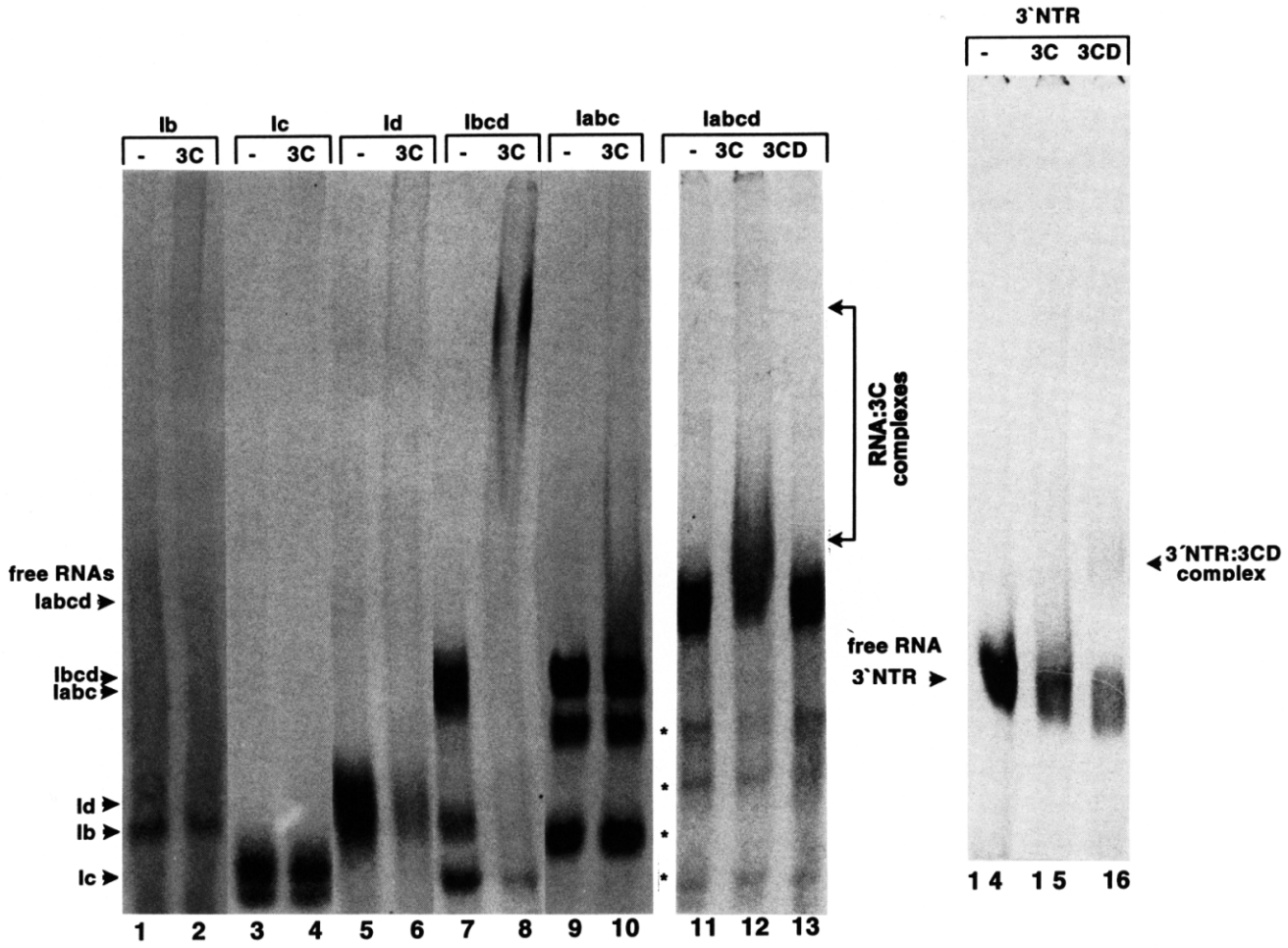

FIGURE 4. Binding of HAV 3C and 3CD to secondary structure elements at the 5′ and 3′ termini of the HAV RNA (see Fig. 2). Electrophoretic mobilities of RNP complexes formed in the presence of HAV $3C^{pro}$ (lanes 8, 10, and 12) or 3CD (lane 16) are indicated. Lanes 15 and 16 show the mobilities of RNAs representing the HAV 3′ NTR in the presence of HAV $3C^{pro}$ or 3CD, respectively. Asterisks indicate the mobility of the prematurely terminated transcripts; "−" denotes the binding reactions performed in the absence of protein.

ious transcripts were tested. Although 3CD was not purified to homogeneity, its RNA binding was found to be specific, because only this protein was labeled predominantly after UV crosslinking and RNase digestion (Fig. 1D, lane 2). Like HAV 3C, 3CD was unable to retard the mobility of small RNAs representing individual secondary structure elements Ia, Ib, Ic, or Id (data not shown). In contrast to 3C, no gel-resolvable complexes were observed after incubation with RNA Ibcd or Iabc (data not shown) and RNA Iabcd (Fig. 4, lane 13). The reverse RNA-binding pattern was found when RNA of the 3′ end was used. Whereas 3C was not able to produce gel-resolvable complexes with the 3′ RNA probe (lane 15), HAV 3CD retarded, albeit not efficiently, the mobility of free RNA (lane 16).

To prove the specificity of HAV 3C^{pro} interaction with the HAV 5′ RNA, competition experiments were performed using unlabeled transcripts that represented secondary structure elements individually or in combination. As shown in Figure 5, the efficiency of crosslinking of radioactive RNA Iabcd to HAV 3C^{pro} was reduced to levels of 70–80% in the presence of unlabeled RNAs representing elements Ia and Ic. Although we showed by mobility shift assay (see above) that RNA structures comprising less than 100 nt did not form stable RNA–protein complexes, we found that RNA Ib, Iab, and Iabc were able to compete for protein binding when they were present at a 200-fold molar excess in the UV crosslinking/label transfer assay. Similar competition was observed, as expected, when Iabcd was used as competitor. A control HAV RNA probe of similar length (105 nt, element II), as well as an unlabeled transcript from pGEM1-mcs, did not compete at all. Based on the results on HAV 3C binding compiled in Figure 2B, it can be concluded that an RNA molecule of more than 100 nt in length and/or containing at least two unique secondary structure elements (such as Ib and Id) is needed for the formation of a stable gel-resolvable RNA–protein complex, implying that interactions at multiple points are involved. Moreover, the competition data (Fig. 5) indicate that stem-loop structures Ib, Iab, and Iabc contribute to specific binding of HAV 3C^{pro} to the secondary structure elements at the 5′ end of the HAV genome.

HAV and HRV14 3C^{pro} binding to picornaviral cloverleaves

A cloverleaf structure formed at the 5′ terminus of the rhino- and poliovirus genomes was shown to interact specifically with the viral proteinase 3C^{pro} or its precursor 3CD^{pro}, respectively (Andino et al., 1990; Harris et al., 1994; Walker et al., 1995). This secondary structure is also required for efficient poliovirus RNA replication (Andino et al., 1993). A similar, yet not identical RNA secondary structure, comprising three stem-loops, was proposed for the 5′ end of the HAV genome (Brown et al., 1991). We compared the 3C binding specificity of

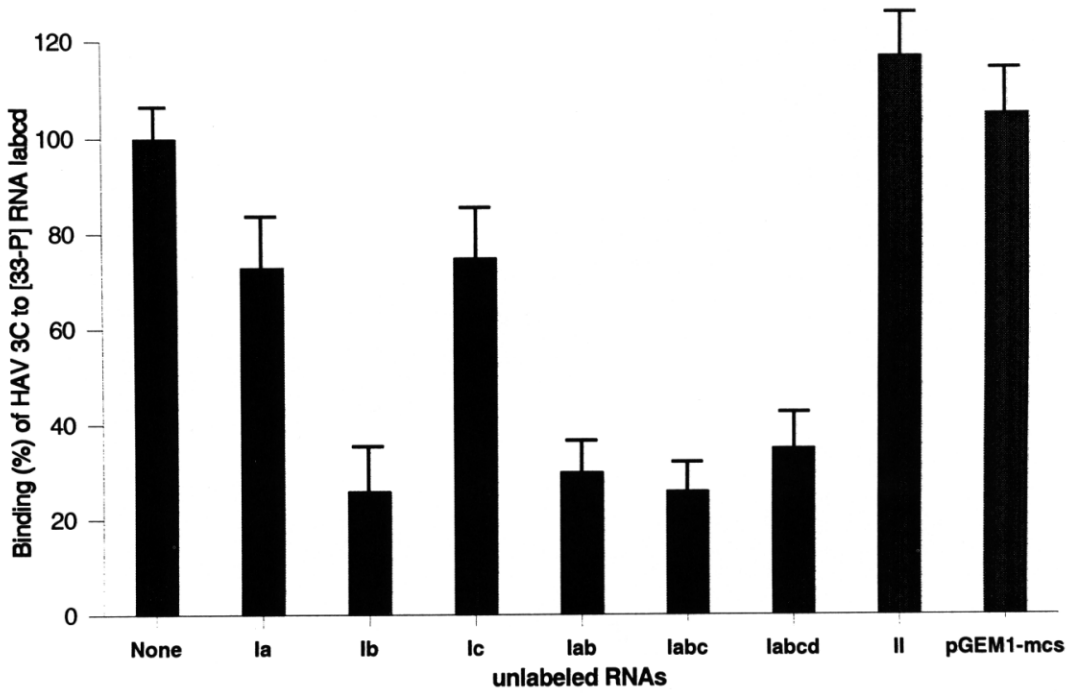

FIGURE 5. Competition for interaction with HAV 3C^{pro} between the radioactive probe Iabcd and unlabeled RNAs representing secondary structure elements individually or in combination (see Fig. 2). The label transfer from RNA probe Iabcd to HAV 3C^{pro}, measured as a signal intensity of crosslinked HAV 3C^{pro}, was taken as 100%. Competing RNAs were used at a 200-fold molar excess. Unlabeled RNA II (nt 151–258) and the transcript from the multiple cloning site of pGEM1 were used as control.

the HAV 5′-terminal RNA structure with that of the cloverleaves of polio and rhinovirus. In addition to HAV $3C^{pro}$, the HRV14 proteinase $3C^{pro}$ was used as a positive control. Whereas both renteroviral cloverleaves formed gel-resolvable complexes with rhinovirus $3C^{pro}$ (Fig. 6B, lanes 3 and 9), such complexes were not observed with HAV $3C^{pro}$ (lanes 2 and 8). Crosslinking of the renteroviral cloverleaves with rhinovirus proteinase 3C was inefficient (Fig. 6A, lanes 3 and 9), as was observed also for polioviral protein 3AB (Xiang et al., 1995b). In the reverse experiment, where the interaction of HAV RNA Iabcd with viral proteinases was tested, the RNA mobility was retarded partially by HAV $3C^{pro}$ (lane 5), as well as by human rhinovirus $3C^{pro}$ (lane 6). Most efficient label transfer from HAV RNA Iabcd was found to cognate HAV $3C^{pro}$, probably reflecting a high extent of physical interaction (Fig. 6A, lane 5). Neither proteinase (HAV or

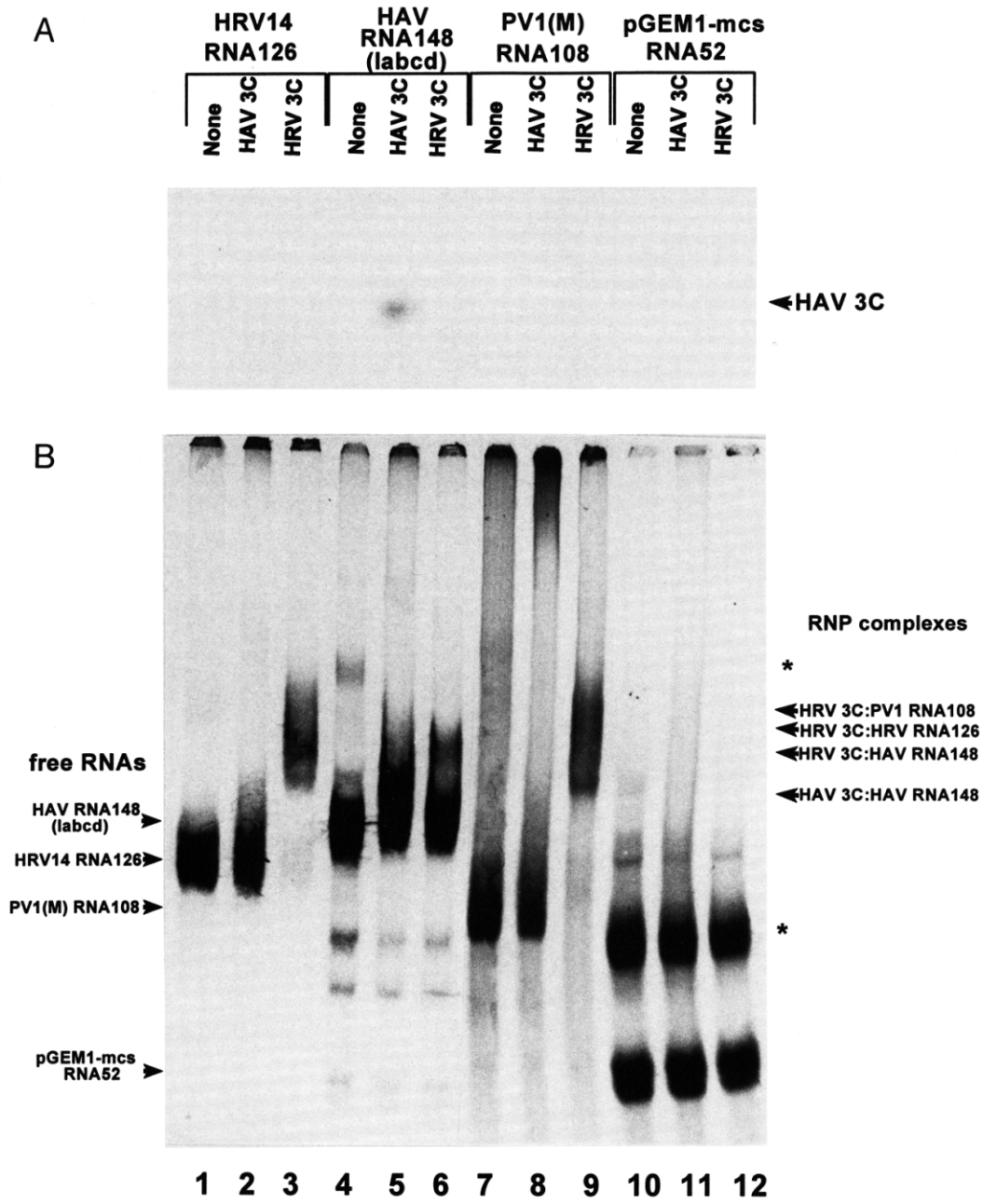

FIGURE 6. Comparison of binding of HAV and HRV14 proteinase 3C to the 5′ secondary structure of picornaviral RNAs. **A:** Label transfer to HAV and HRV14 $3C^{pro}$ from HRV14 RNA 126 (lanes 2 and 3), HAV RNA 148 (element Iabcd, lanes 5 and 6), and poliovirus RNA 108 (lanes 8 and 9) and the transcript of pGEM1-mcs (lanes 11 and 12). **B:** Electrophoretic mobility of free RNA probes (lanes 1, 4, 7, and 10, shown by arrow heads at the left) and RNP complexes with HRV14 $3C^{pro}$ (lanes 3, 6, and 9) or HAV $3C^{pro}$ (lane 5, indicated at the right). Asterisks denote alternative secondary or high-order structures of radioactive transcripts.

HRV14 3C^{pro}) reacted well with an RNA probe transcribed from the multiple cloning site of pGEM1, demonstrating that vector-derived nucleotides are not involved in the interaction (lanes 10–12). These data confirm earlier reports showing that rhinovirus 3C^{pro} interacts strongly not only with the cognate 5′ cloverleaf-like structure, but also with the secondary structure elements at the 5′ end of the poliovirus RNA, implying that these cloverleaves are very similar and interchangeable (Walker et al., 1995; Xiang et al., 1995b). In addition, these results demonstrate that HRV14 3C^{pro} can also interact, albeit not efficiently, with secondary structure elements at the 5′ end of the HAV RNA (Fig. 6B, lane 6). In close agreement with previously published data (Brown et al., 1991), the lack of HAV 3C^{pro} binding to renteroviral cloverleaves (Fig. 6, lanes 2 and 8) implies that the 5′ end of HAV RNA may fold into a secondary or high-order structure different from that of the rhino- and poliovirus cloverleaf.

DISCUSSION

In the past years, the proteolytic properties of HAV proteinase 3C^{pro} have been studied in great detail (Gauss-Müller et al., 1991; Jia et al., 1991; Harmon et al., 1992; Kusov et al., 1992; Schultheiss et al., 1995). These results underlined the central role that the viral proteinase plays in the early phase of the viral life cycle when protein synthesis dominates. The step presumed to follow next is the replication of the viral genome, which seems to require the function of all viral nonstructural proteins in concert with not yet identified host factors. For poliovirus, genetic evidence suggested that the major viral proteinase also takes part in this process and may thus exert additional functions (Andino et al., 1993). Multiple functions of other picornaviral proteins have been described recently and have shed light on the economic usage of the picornaviral genome (see Wimmer et al., 1993 for review). Here we present first evidence that the proteinase 3C^{pro} of HAV, like polio- and rhinovirus 3C^{pro} or 3C^{pro}-containing polypeptides, can bind specifically to its cognate RNA.

Amino acid sequence alignment does not allow to classify the picornaviral 3C proteinases among the RNA-binding proteins, yet most of them contain a highly conserved amino acid sequence motif (KFRDI) that connects the two β-barreled domains of the enzyme (Gorbalenya et al., 1989; Allaire et al., 1994; Matthews et al., 1994). Detailed genetic analysis of polio and rhinovirus 3C^{pro} showed that mutations among the amino acid residues of the domain connection, in the β-sheets B1, C1, the TGK motif C-terminal to the active site cysteine, and near the C terminus abolish the RNA-binding capacity of 3C, whereas mutations in the catalytic triad had no impact on RNA interaction (Hammerle et al., 1992; Walker et al., 1995; Blair et al., 1996). Most of the basic and hydrophobic residues involved in RNA binding are located opposite to the active site where the catalytic center is positioned (Matthews et al., 1994). Our observation that the proteolytically inactive mutant of the HAV 3C interacts with RNA as efficiently as the wild-type enzyme supports the notion that the catalytic and RNA-binding domains are at separate locations on the 3C surface and may reflect independent functions of HAV 3C^{pro} in viral RNA replication and in polyprotein processing.

Initial analysis of the RNA-binding specificity of HAV 3C^{pro} revealed that RNA transcripts comprising more than 150 nt interacted efficiently with the proteinase, yet in a rather unspecific manner. Besides the RNA probes derived from the HAV 5′ NTR, highly structured transcripts of the EMCV IRES (585 nt) or the 3′ end of the HAV genome (502 nt) bound to HAV and rhinovirus 3C (data not shown). RNA transcripts of less than 100 bases length did not interact with HAV 3C^{pro} in a thermodynamically stable fashion because the proteinase was not able to retard the RNAs' electrophoretic mobility. Although none of the individual stem-loop structures and the combinations Iab and Iabc resulted in stable gel-resolvable complexes with 3C, most of them competed for binding with element Iabcd. These conflicting observations can be reconciled by considering that the mobility shift assay, being a nonequilibrium method, detects only gel-resolvable complexes (Weeks et al., 1992). Thus, using this assay, a bias is introduced against interactions not stable to complex isolation (see Cann, 1989; Lane et al., 1992). However, competition of individual structural elements detected by label transfer after UV crosslinking reflects RNA binding at equilibrium status and therefore the extent of physical interaction between the RNA and HAV proteinase 3C^{pro}. Taking the data on mobility shift and competition experiments together, we conclude that individual secondary structure elements at 5′ end of the HAV RNA interact with the protein and contribute to the RNA-binding specificity of HAV 3C^{pro}. However, a thermodynamically stable RNP complex is only formed when RNA molecules of a large size (more than 100 nt), which contain, in addition, two unique secondary structure elements (Ib and Id), interact with the protein, probably involving multiple point interactions. Whereas no stable interaction of any individual stem-loop structure of either element I (Ia, Ib, Ic, and Id) was detected for HAV 3C^{pro}, rhinovirus 3C was shown to retard the mobility of its own cloverleaf (see Fig. 6) and also to shift the mobility of the individual stem-loop "d" (Walker et al., 1995). These interaction studies were performed under high ionic strength, which might stabilize particular RNA structures and thus facilitate RNP complex formation. It is also interesting to note that the abovementioned consensus sequence for RNA binding differs slightly for either proteinase when the adjacent amino acids are

included (78-RNE**KFRDI**R-86 in HRV14 $3C^{pro}$ and 92-TIP**KFRDI**T-100 in HAV $3C^{pro}$). Furthermore, other regions at the back side of $3C^{pro}$ that surround this motif and presumably bind to viral RNA are different in both proteinases (Allaire et al., 1994; Matthews et al., 1994). Whether this difference can affect the efficiency of the RNA binding has to be elucidated.

The overall weak RNA-binding activity of picornaviral 3C proteinases requires relatively high enzyme concentration in binding assays. Similar to what has been reported for rhinovirus proteinase $3C^{pro}$ (Leong et al., 1993; Walker et al., 1995), we found that HAV $3C^{pro}$ reacted efficiently with RNA at a concentration of approximately 8 μM. Rather weak RNP complex formation was also shown for poliovirus $3C^{pro}$ (Andino et al., 1990). The formation of the poliovirus RNP complex was improved significantly by the addition of small amounts of 3Dpol or 3AB to the binding reaction (Harris et al., 1994). Moreover, RNA binding was more pronounced for the poliovirus precursor protein $3CD^{pro}$ compared to the mature proteinase 3C or polymerase 3D (Andino et al., 1993). These data, as well as genetic evidence, supported the notion that RNA binding by these polypeptides is conferred by the 3C moiety, whereas additional regions of the precursor protein serve to improve the RNA-binding specificity (Andino et al., 1993; Xiang et al., 1995b). In contrast to poliovirus, we show that binding of HAV RNA of the 5′ NTR was not improved when similar concentrations of 3CD were used instead of 3C, suggesting that the 3D moiety does not affect the RNA-binding specificity of HAV 3C. It is interesting to note that HAV 3CD, unlike poliovirus 3CD, was not detected as a predominant product of polyprotein processing. Instead, HAV 3ABC was found to be a relatively stable intermediate when the HAV polyprotein was translated in vitro or expressed in bacteria and mammalian cells (Harmon et al., 1992; Schultheiss et al., 1994). We are currently pursuing experiments to answer the question of whether HAV 3ABC exhibits altered RNA-binding specificities or whether host factors or viral proteins can affect the binding of HAV 3C and/or its precursors.

MATERIALS AND METHODS

Expression and purification of HAV 3C and 3CD

HAV $3C^{pro}$ and its proteolytically inactive mutant 3Cμ (C24S and C172A) expressed in *E. coli* BL21 (DE3) were purified by ion-exchange chromatography and detected by silver staining and immunoblot as described previously (Malcolm et al., 1992; Schultheiss et al., 1995). $3C^{pro}$ of rhinovirus (HRV) 14 was kindly provided by B. Malcolm. His-tagged and proteolytically inactive 3CD was a product of pET15-3CDμ, which was generated by inserting the mutated (C172A) 3CD fragment derived from pET-3CD into pET15b (Kusov et al., 1992). The nucleotide sequence of the plasmid was verified by sequencing. Using a nickel affinity column, bacterially expressed HAV 3CD was purified partially from the soluble fraction according to the manufacturer's protocol (Qiagen).

RNA probes

pT7-HAV1 and pHAV/7, both bearing the sequence of the attenuated HAV strain HM175, were used as source of RNA transcripts comprising various parts of the HAV 5′ NTR (Cohen et al., 1987; Harmon et al., 1991). After linearization with *Nco* I and transcription using T7 RNA polymerase, pT7-HAV1 gave rise to an RNA comprising nt 1–45 (the nucleotide numbering of wild-type HAV strain HM175 is used throughout) and representing the 5′ NTR structural element Ia. pHAV/7 was linearized with *Avr* II, *Ssp* I, *Hae* III, *Hpa* I, and *Xba* I before transcription with SP6 RNA polymerase to yield RNA probes covering nt 1–81 (Iab), 1–148 (Iabcd), 1–259 (elements I–II), 1–354 (elements I–III), and 1–744 (complete 5′ NTR, elements I–V), respectively. To obtain 5′ progressively deleted transcripts containing nt 46–744 (Ib–V), 151–744 (II–V), 355–744 (IV–V), 447–744 (IV*–V, * designates partial sequences), 533–744 (V), and 634–744 (V*), plasmids pΔ46, pΔ151, pΔ355, pΔ447, pΔ534, and pΔ634, respectively, bearing the sequence of the wild-type strain HM175 of HAV (Brown et al., 1991), were linearized with *Xba* I and used as template for transcription with SP6 RNA polymerase. Some of these plasmids, after linearization with appropriate enzymes (*Avr* II and *Ssp* I for pΔ46, *Avr* II and *Hpa* I for pΔ151, *Nsi* I for pΔ355) and transcription with SP6 RNA polymerase, produced RNA probes, representing stem-loop Ib (nt 46–81), stem-loop Ibcd (nt 46–148), element II (nt 151–248), elements II–III (nt 151–354), and element IV (nt 355–532), respectively. To generate the RNA probe representing nt 1–95 (element Iabc) of the HAV genome, plasmid pGEM1-HM1-95 was constructed by PCR amplification using pHAV/7 as template and the primers 5′-tgtcgttagaacgcggctacaattaatacat aaccttat-3′ (sense, located upstream of the SP6-promotor at nucleotide position 2794–2836 of pGEM1) and 5′-gc**gaattc** AGCCTATAGCCTAGGCAAACGG-3′ (antisense, carrying an *Eco*R I restriction site, shown in bold, adjacent to the HAV sequence complementary to nt 95–74, shown in capital letters). The PCR-fragment was restricted with *Eco*R I and *Hin*d III and inserted into pGEM1 cut with the same enzymes. The RNA element Iabc was transcribed after complete linearization of pGEM1-HM1-95 with *Eco*R I. To transcribe stem-loop Ic separately, pGEM1-HM1-95 was modified by restriction with *Hin*d III and *Avr* II, filling in with Klenow enzyme, and religation. After linearization of the resulting plasmid pGEM1-HM81-95 with *Eco*R I followed by transcription with SP6 RNA polymerase, the RNA element Ic was prepared. To generate the polypyrimidine tract (element Id or pYI), pGEM1-HM96-744 was constructed by PCR amplification using pHAV/7 as template and primers 5′-tac**aagctt** AAATTTTCCCTTTCCCTTTTCCC-3′ (sense, *Hin*d III site in bold; HAV sequences, nt 96–118) and 5′-TTG**TCTAGA**CAT GTTCATTATTATTTAAGAATGAGG-3′ (antisense, *Xba* I site in bold; HAV sequences, nt 747–712). The PCR fragment was cut with *Hin*d III and *Xba* I and ligated into pGEM1 restricted with the same enzymes. Following linearization of pGEM1-HM96-744 with *Ssp* I (nt 148) and transcription with SP6 RNA polymerase, secondary structure element Id was

generated. The preparation of transcripts of the 3′ end of the HAV genome was described earlier (Kusov et al., 1996). To produce the RNA probes representing the 5′ cloverleaves of polio and HRV14, pT7PV(M) or pLJ5NCR1 were linearized with *Hga* I or *Hin*d III, respectively, and transcribed with T7 RNA polymerase (van der Werf et al., 1986; Leong et al., 1993). The size and genome localization of all transcripts is shown in Figure 2. Unlabeled RNA probes were synthesized using the MEGAscript kit, according to manufacturer's protocol (Ambion). To prepare radioactively labeled RNA transcripts [α-^{33}P]UTP (2,000 Ci/mmol, NEN DuPont) was used in the MAXIscript SP6/T7 kit (Ambion). Unincorporated nucleotides were removed by two successive ethanol precipitations. In some experiments, the radioactive transcripts were gel-purified as described previously (Kusov et al., 1996).

RNA gel shift analysis

RNA–protein binding reactions were performed as described previously (Chang et al., 1993; Kusov et al., 1996). Briefly, a 60-μL reaction mixture containing ^{33}P-labeled RNA (0.5–1 × 105 cpm) and 3–10 μg of protein in binding buffer (5 mM HEPES (*N*-2-hydroxyethylpiperazine-*N*′-ethansulfonic acid), pH 7.9, 25 mM KCl, 2 mM $MgCl_2$, 1.75 mM ATP, 6 mM DTT, 0.05 mM phenylmethylsulfonyl fluoride (PMSF), 166 μg/mL of *E. coli* tRNA and 5% glycerol) was incubated for 20 min at 30 °C. An aliquot of 15 μL was withdrawn from the reaction mixture, supplemented with 5 μL of sample buffer (1 mM EDTA, 0.25% bromophenol blue, 0.25% xylene cyanol, 50% glycerol) and analyzed on a 5% nondenaturing polyacrylamide gel that had been prerun for 60 min at 4 °C and 80 V. Electrophoresis was conducted at 200 V at 4 °C until the bromophenol blue marker had migrated to a position of 1/2–2/3 of the gel length, depending on the size of the RNA probe. The gels were dried and subjected to autoradiography. In competition experiments, the unlabeled RNA (approximately 200-fold molar excess) was incubated for 20 min at 30 °C with the components of the binding mixture described above prior to the addition of the radioactive RNA probe and further incubation for 20 min.

UV crosslinking/label transfer

The remainder (45 μL) of the above-described RNA–protein binding reaction was transferred to a flat-bottom 96-well plate and irradiated with UV (254 nm) on ice for 45 min at a distance of 2–4 cm (Stratalinker 1800). Subsequently, RNA was digested with 20 μg of RNase A and 20 U of RNase T1 at 37 °C for 15 min. The UV-crosslinked products were separated by discontinuous SDS-PAGE. The gels were fixed, dried, amplified, and exposed to X-ray film at −70 °C with intensifying screen. The intensity of the bands was quantitated with an OPTOQUANT (Computer & Vision, Lübeck) using slightly exposed films.

Northwestern analysis of the RNA-3C complex

Detection of HAV 3C by northwestern analysis was performed essentially as described (Blackwell & Brinton, 1995). Briefly, purified HAV 3C (approximately 5 μg) was separated by SDS-PAGE and transferred onto nitrocellulose (Schleicher & Schüll). The membrane was blocked at room temperature for 1 h with PBS containing 5% nonfat milk and 1 mM DTT and then washed with 1× HBB (25 mM HEPES-KOH, pH 7.5, 25 mM NaCl, 5 mM $MgCl_2$, and 1 mM DTT). The transferred protein was renatured by consecutive washes (15 min each at room temperature) with 6, 3, 1.5, 0.75, 0.375, 0.187, and, finally, 0 M guanidinium hydrochloride in 1× HBB. The membrane was washed twice with 1× HYB (20 mM HEPES-KOH, pH 7.5, 100 mM KCl, 2.5 mM $MgCl_2$, 0.1 mM EDTA, 0.05% Nonidet P-40, and 1 mM DTT) and once with 1× HYB containing *E. coli* tRNA (1 μg/mL). ^{33}P-labeled RNA I–V (2 × 105 cpm/mL, see Fig. 2) in 1× HYB, containing tRNA (1 μg/mL) and RNasin (1 U/mL) was incubated with the renatured membrane-bound protein for 1 h at room temperature and then overnight at 4 °C. Unbound probe was removed by three washes with 1× HYB. The membrane was dried at room temperature and autoradiographed. For the subsequent immune reaction, anti-3C antibody raised in rabbits against recombinant HAV 3C^{pro} was used (Gauss-Müller et al., 1991).

ACKNOWLEDGMENTS

We thank Ms. S. Schwindt for technical assistance and Drs. R. Hartmann and P.K. Müller for stimulating discussions and critical reading of the manuscript. Some cDNA constructs and purified HRV14 3C^{pro} were generously provided by Drs. S. Lemon, A. Porter, A. Paul, and B. Malcolm. This work was supported by the German Research Society (DFG) within the SFB 367, project B7.

Received August 5, 1996; returned for revision September 25, 1996; revised manuscript received December 3, 1996

REFERENCES

Allaire M, Chernaia MM, Malcolm BA, James MNG. 1994. Picornaviral 3C cysteine proteinases have a fold similar to chymotrypsin-like serine proteinases. *Nature 369*:72–76.

Andino R, Rieckhof GE, Achacoso PL, Baltimore D. 1993. Poliovirus RNA synthesis utilizes an RNP complex formed around the 5′-end of viral RNA. *EMBO J 12*:3587–3598.

Andino R, Rieckhof GE, Baltimore D. 1990. A functional ribonucleoprotein complex forms around the 5′ end of poliovirus RNA. *Cell 63*:369–380.

Bazan EZ, Fletterick RJ. 1988. Viral cysteine proteases are homologous to the trypsin-like family of serine proteases: Structural and functional implications. *Proc Natl Acad Sci USA 85*:7872–7876.

Blackwell JL, Brinton MA. 1995. BHK cell proteins that bind to the 3′ stem-loop structure of the West Nile virus genome RNA. *J Virol 69*:5650–5658.

Blair WS, Nguyen JHC, Parsley TB, Semler BL. 1996. Mutations in the poliovirus 3CD proteinase S1-specificity pocket affect substrate recognition and RNA binding. *Virology 218*:1–13.

Borman AM, Bailly JL, Girard M, Kean KM. 1995. Picornaviral internal ribosome entry segments: Comparison of translation efficiency and the requirements for optimal internal initiation of translation in vitro. *Nucleic Acids Res 23*:3656–3663.

Brown EA, Day SP, Jansen RW, Lemon SM. 1991. The 5′ nontranslated region of hepatitis A virus RNA: Secondary structure and elements required for translation in vitro. *J Virol 65*:5828–5838.

Brown EA, Zajac AJ, Lemon SM. 1994. In vitro characterization of an internal ribosomal entry site (IRES) present within the 5′ nontranslated region of hepatitis A virus RNA: Comparison with the IRES of encephalomyocarditis virus. *J Virol 68*:1066–1074.

Cann JR. 1989. Phenomenological theory of gel electrophoresis of protein–nucleic acid complexes. *J Biol Chem 264*:17032–17040.

Carneiro JS, Equestre M, Pagnotti P, Gradi A, Sonenberg N, Berkoff RP. 1995. 5′ UTR of hepatitis A virus RNA: Mutations in the 5′-most pyrimidine-rich tract reduce its ability to direct internal initiation of translation. *J Gen Virol 76*:1189–1196.

Chang KH, Brown EA, Lemon SM. 1993. Cell type-specific proteins which interact with the 5′ nontranslated region of hepatitis A virus RNA. *J Virol 67*:6716–6725.

Cohen JI, Ticehurst JR, Feinstone SM, Rosenblum B, Purcell RH. 1987. Hepatitis A virus cDNA and its RNA transcripts are infectious in cell culture. *J Virol 61*:3035–3039.

Gauss-Müller V, Jürgensen D, Deutzman R. 1991. Autoproteolytic cleavage of recombinant 3C proteinase of hepatitis A virus. *Virology 182*:861–864.

Gorbalenya AE, Donchenko AP, Blinov VM, Koonin EV. 1989. Cysteine proteases of positive strand RNA viruses and chymotrypsin-like serine proteases: A distinct protein superfamily with a common structural fold. *FEBS Lett 243*:103–114.

Hahn H, Palmenberg AC. 1995. Encephalomyocarditis viruses with short poly(C) tracts are more virulent than their mengovirus counterparts. *J Virol 69*:2697–2699.

Hammerle T, Molla A, Wimmer E. 1992. Mutational analysis of the proposed FG loop of poliovirus proteinase 3C identifies amino acids that are necessary for 3CD cleavage and might be determinants of a function distinct from proteolytic activity. *J Virol 66*:6028–6034.

Harmon SA, Richards OC, Summers DF, Ehrenfeld E. 1991. The 5′ terminal nucleotides of hepatitis A virus RNA, but not poliovirus RNA, are required for infectivity. *J Virol 65*:2757–2760.

Harmon SA, Updike W, Jia XY, Summers DF, Ehrenfeld E. 1992. Polyprotein processing in *cis* and in *trans* by hepatitis A virus 3C protease cloned and expressed in *Escherichia coli*. *J Virol 66*:5242–5247.

Harris KS, Xiang W, Alexander L, Lane WS, Paul AV, Wimmer E. 1994. Interaction of poliovirus polypeptide $3CD^{pro}$ with the 5′ and 3′ termini of the poliovirus genome. *J Biol Chem 269*:27004–27014.

Jackson RJ. 1989. Comparison of encephalomyocarditis virus and poliovirus with respect to translation initiation and processing in vitro. In: Semler BL, Ehrenfeld E, eds. *Molecular aspects of picornavirus infection and detection*. Washington, DC: American Society for Microbiology. pp 51–71.

Jacobson SJ, Konings DAM, Sarnow P. 1993. Biochemical and genetic evidence for a pseudoknot structure at the 3′ terminus of the poliovirus RNA genome and its role in viral RNA amplification. *J Virol 67*:2961–2971.

Jia XY, Ehrenfeld E, Summers DF. 1991. Proteolytic activity of hepatitis A virus 3C protein. *J Virol 65*:2595–2600.

Kusov Y, Sommergruber W, Schreiber M, Gauss-Müller V. 1992. Intermolecular cleavage of hepatitis A virus (HAV) precursor protein P1-P2 by recombinant HAV proteinase 3C. *J Virol 66*:6794–6796.

Kusov Y, Weitz M, Dollenmeier G, Gauss-Müller V, Siegl G. 1996. RNA–protein interactions at the 3′ end of the hepatitis A virus RNA. *J Virol 70*:1890–1897.

Lane D, Prentki P, Chandler M. 1992. Use of gel retardation to analyse protein-nucleic acid interactions. *Microbiol Rev 56*:509–528.

Le SY, Chen JH, Sonenberg N, Maizel JV. 1993. Conserved tertiary structural elements in the 5′ nontranslated region of cardiovirus, aphthovirus and hepatitis A virus RNAs. *Nucleic Acids Res 21*:2445–2451.

Leong LEC, Walker PA, Porter A. 1993. Human rhinovirus-14 protease 3C ($3C^{pro}$) binds specifically to the 5′-noncoding region of the viral RNA. *J Biol Chem 268*:25735–25739.

Malcolm BA, Chin SM, Kewell DA, Stratton-Thomas JR, Thudium KB, Ralston R, Rosenberg S. 1992. Expression and characterization of recombinant hepatitis A virus 3C proteinase. *Biochemistry 31*:3358–3363.

Martin LR, Duke GM, Osorio JE, Hall DJ, Palmenberg AC. 1996. Mutational analysis of the mengovirus poly(C) tract and surrounding heteropolymeric sequences. *J Virol 70*:2027–2031.

Matthews DA, Smith WW, Ferre RA, Condon B, Budahazi G, Sisson W, Villafranca JE, Janson Ca, McElroy HE, Gribskov CL, Worland S. 1994. Structure of human rhinovirus 3C protease reveals a trypsin-like polypeptide fold, RNA-binding site, and means for cleaving precursor polyprotein. *Cell 77*:761–771.

Percy NW, Barclay WS, Sullivan M, Almond JW. 1992. A poliovirus replicon containing the chloramphenicol acetyltransferase gene can be used to study the replication and encapsidation of poliovirus RNA. *J Virol 66*:5040–5046.

Rohll JB, Percy N, Ley R, Evans DJ, Almond JW, Barclay WS. 1994. The 5′-untranslated regions of picornavirus RNAs contain independent functional domains essential for RNA replication and translation. *J Virol 68*:4384–4391.

Rueckert RR. 1996. Picornaviridae: The viruses and their replication. In: Fields BN, Knipe DM, Howley PM et al., eds. *Virology*. Philadelphia: Raven. pp 609–654.

Schultheiss T, Kusov YY, Gauss-Müller V. 1994. Proteinase 3C of hepatitis A virus (HAV) cleaves the HAV polyprotein P2-P3 at all sites including VP1/2A and 2A/2B. *Virology 198*:275–281.

Schultheiss T, Sommergruber W, Kusov Y, Gauss-Müller V. 1995. Cleavage specificity of purified recombinant hepatitis A virus 3C proteinase on natural substrates. *J Virol 69*:1727–1733.

Schultz DE, Hardin CC, Lemon SM. 1996. Specific interaction of glyceraldehyde 3-phosphate dehydrogenase with the 5′ nontranslated RNA of hepatitis A virus. *J Biol Chem 271*:14134–14142.

Shaffer DR, Brown EA, Lemon SM. 1994. Large deletion mutations involving the first pyrimidine-rich tract of the 5′ nontranslated RNA of human hepatitis A virus define two adjacent domains associated with distinct replication phenotypes. *J Virol 68*:5568–5578.

Shaffer DR, Lemon SM. 1995. Temperature-sensitive hepatitis A virus mutants with deletions downstream of the first pyrimidine-rich tract of the 5′ nontranslated RNA are impaired in RNA synthesis. *J Virol 69*:6498–6506.

Walker PA, Leong LEC, Porter AG. 1995. Sequence and structural determinants of the interaction between the 5′-noncoding region of picornaviral RNA and rhinovirus protease 3C. *J Biol Chem 270*:14510–14516.

Weeks KM, Crothers DM. 1992. RNA binding assay for Tat-derived peptides: Implication for specificity. *Biochemistry 31*:10281–10287.

van der Werf S, Bradley J, Wimmer E, Studier FW, Dunn JJ. 1986. Synthesis of infectious poliovirus RNA by purified T7 RNA polymerase. *Proc Natl Acad Sci USA 83*:2330–2334.

Whetter LE, Day SP, Elroy-Stein O, Brown EA, Lemon SM. 1994. Low efficiency of the 5′ nontranslated region of hepatitis A virus RNA in directing cap-independent translation in permissive monkey kidney cells. *J Virol 68*:5253–5263.

Wimmer E, Hellen CUT, Cao X. 1993. Genetics of poliovirus. *Annu Rev Genet 27*:353–436.

Xiang W, Cuconati A, Paul AV, Cao X, Wimmer E. 1995a. Molecular dissection of the multifunctional poliovirus RNA-binding protein 3AB. *RNA 1*:892–904.

Xiang W, Harris KS, Alexander L, Wimmer E. 1995b. Interaction between the 5′ terminal cloverleaf and $3AB/3CD^{pro}$ of poliovirus is essential for RNA replication. *J Virol 69*:3658–3667.

Ypma-Wong MF, Dewalt PG, Johnson VH, Lamb JG, Semler BL. 1988. Protein 3CD is the major poliovirus proteinase responsible for cleavage of the P1 capsid precursor. *Virology 166*:265–270.